

SYNTHETIC MODELLING OF SEISMIC REFLECTIONS FROM MIOCENE SANDS, ONSHORE TARANAKI

D J Woodward¹ and C Stone²

¹Institute of Geological and Nuclear Sciences Ltd, P O Box 1320, Wellington

²New Zealand Oil and Gas Ltd, Wellington

Abstract

The marine Miocene and Pliocene formations of the onshore Taranaki Basin, generally an alternating sand-shale sequence, exhibit high seismic reflectivity that offers good structural resolution for petroleum exploration. Synthetic modelling based on the sequence in the Burgess-1 exploration well, Cape Egmont, shows that the efficiency in compressional (P) wave to shear (SV) wave conversion is strongly influenced by the porosity and hence the density of the sandstones. Poisson's ratio also has a marked effect on the strength of the reflections and converted waves.

The modelling undertaken, using a full wave equation technique that accommodates variations in porosity and permeability of the strata, has shown that the converted waves could theoretically be recorded using three component geophones. However, the identification of such waves depends on the ability to isolate these events from the many reflections from within the highly reflective Miocene-Pliocene sequence. If this separation can be achieved it may offer important insights into the properties of the rocks and their interstitial fluids, and so aid exploration programmes.

A walkout test has been undertaken near the Burgess-1 exploration well using explosives as an energy source and recording the data on three component (orthogonal) geophones. The results of converted wave modelling compare well with the vertical component geophones of the walkout test. However, low signal to noise ratios on the horizontal geophones and the difficulty in effective separation of SV waves significantly impede resolving the complex lithologies on these records.

Introduction

Geology

The Taranaki Basin is a thick Cretaceous-Cenozoic clastic wedge lying beneath New Zealand's western continental margin. The basin comprises two structural regions, the stable western margin and the faulted depression, containing up to 11,000 m³ of clastic sediments, termed the Taranaki Graben. The Taranaki Basin was formed by Late Cretaceous to Paleocene rifting associated with the continental breakup of Gondwana, followed by gradual subsidence resulting in widespread deposition of non-marine, paralic and marine sediments and the development of a foreland basin. Compressional tectonism commenced in the Oligocene, resulting in rapid subsidence of the foredeep in the east and, by the early Miocene rapid deposition of clastic material sourced from the proto-Southern Alps was occurring. Towards the end of the Miocene compressional tectonics were replaced by extension associated with back-arc spreading. This resulted in renewed subsidence and sedimentation which continued until the late Pliocene when a dextral strike-slip duplex regime was imposed. This continues today.

Early petroleum exploration in the area focussed on objectives closely related to the source rocks (the Eocene Kapuni Group). This was because the sequence is associated with a strong, regionally mappable seismic marker, and because early discoveries were within this sequence. The shallower clastic sequence was therefore overlooked until the recent Kaimaro and Ngatoro discoveries. The reservoirs in these discoveries are high porosity (20-30%), moderately permeable (50 to 1000 mD), deep marine clastics, mainly comprising turbidite fans and lobes. These sands have (to date) provided flow rates of up to 600 bbls/day. Considerable exploration potential remains in these Miocene Moki and Mt Messenger formations and Pliocene Mangaa and Urenui formations.

Seismic character of the Miocene-Pliocene sand sequence

The apparent seismic reflectivity of the Miocene-Pliocene sequence varies, in part due to regional lithological variations, but more significantly due to surface geology. The seismic data quality in much of west Taranaki — including the study area near Cape Egmont (figure 1) — is excellent, providing images of a moderately reflective sequence. In the past the seismic reflectivity within the prospective sequence has

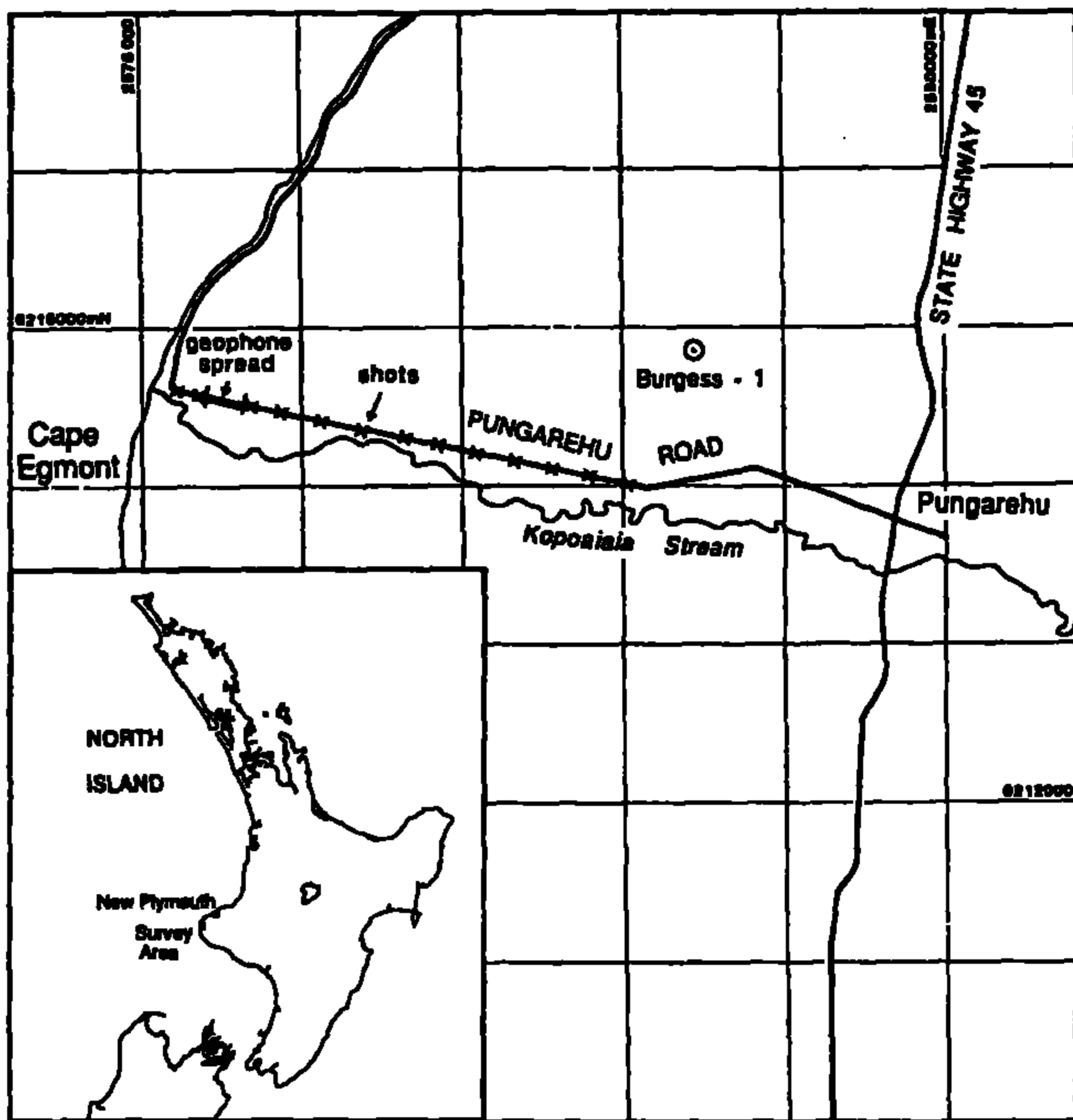


Fig. 1. Location and configuration for the walkout test at Cape Egmont, Taranaki, New Zealand.

been assumed to be largely due to density-derived impedance contrasts within the interbedded sands and shales (with little acoustic compressional velocity contrast). However, some of the reflectivity within the sequence is shown in this paper to be due to variations in Poisson's ratio and hence shear wave velocities.

Reflections at an interface with porous media considerations

There are three types of seismic wave that are important in a porous medium such as a sandstone. These are the shear wave (S) and two compressional waves — one mainly associated with the solid matrix (Type I wave) and the other with the fluid filling the pores (Type II waves). The relationship between these waves has been discussed in detail by many workers (e.g. Bourbie et al 1987, White, 1983). The velocity of the waves depend not only on the properties of the rock matrix, and the fluid but also on the frequency of the seismic waves.

When a seismic wave is incident on an interface between differing porous materials six new seismic waves result (3 reflected waves and 3 transmitted waves). In general all these waves have different frequency dependent velocities. The Type-II waves are generally ignored in seismic reflection studies as they are highly attenuated and so seldom directly observed. However, in some cases (e.g. Woodward and Haines, 1992) their effect can be significant in that their generation modifies the partitioning of seismic energy between the S and Type-I waves transmitted and reflected at the interfaces.

Previous uses of converted wave data

Studies involving phase converted waves have traditionally considered waves that are caused by explosive seismic sources in non-porous media (Type-I waves) and are recorded at the surface as shear waves.

These studies have generally concentrated on the determination of the shear wave velocity which when combined with the compressional wave velocities provide an estimate of the Poisson's ratio structure of the strata (e.g.

Lawton and Harrison (1990)) and the variation of signal with the fluids in the rocks (e.g. Ensley, 1984, Robertson and Pritchett, 1986).

With the often poor compressional wave impedance contrasts between the shales and very fine sands of the Taranaki Miocene sequences it was considered that variations in the P to S conversion of seismic waves may be useful in defining the sand and shale layers and thus providing an indicator of the variation of the porosity (and hence prospectivity) of the sands.

Geology of Burgess-1 exploration well

The Burgess-1 exploration well was drilled to 3264 m bdf by NZOG (operating for the PPL38702 Joint Venture) in 1989. Burgess-1 sought to test the hydrocarbon potential of the regressive marine sequence of Miocene and Pliocene age on a seismically defined horst. Although the well encountered sandstone beds up to 50 m thick, with porosities up to 35%, and core permeabilities up to 1 Darcy, no hydrocarbon shows were indicated.

The stratigraphy of the Burgess-1 well is shown in table 1 and in figure 2.

Synthetic Reflections from the Miocene Sands

The synthetic shot records were computed using a full wave field propagation method developed within the Institute for horizontally layered models. The model is based on the following assumptions:

- The strata are laterally homogeneous.
- The seismic velocities are those of a porous medium and follow the mathematical relationships expressed in Bourbie et al (1987).
- The seismic velocities and permeability are isotropic.
- Cylindrical waves fields are considered. This will cause a small departure from the results that may be expected in any field observations but it is believed the errors would be small compared with the uncertainties due to departures from the other assumptions and noise on the observed records.
- For the computations in this study it is assumed that the (explosive) sources are below the receivers. The direct waves from the source to receivers are ignored as are the effects of the free surface.

Table 1. Geology of the Burgess-1 well.

Depth (m bgs)	Formation	Description
0-82	Egmont Volcanics	Quaternary volcanic agglomerates
82-1194	Kahawai Beds	Sand-rich outer to middle shelf
1194-1560	Giant Foresets	Shale dominated slope sequence
1560-2103	Mangaa	Early Pliocene bathyal interbedded sandstones and shales
2103-2604	Mt Messenger	Late Miocene bathyal interbedded sandstones and shales
2604-3255	Manganui	Mid-late Miocene bathyal shales with minor interbedded sandstones

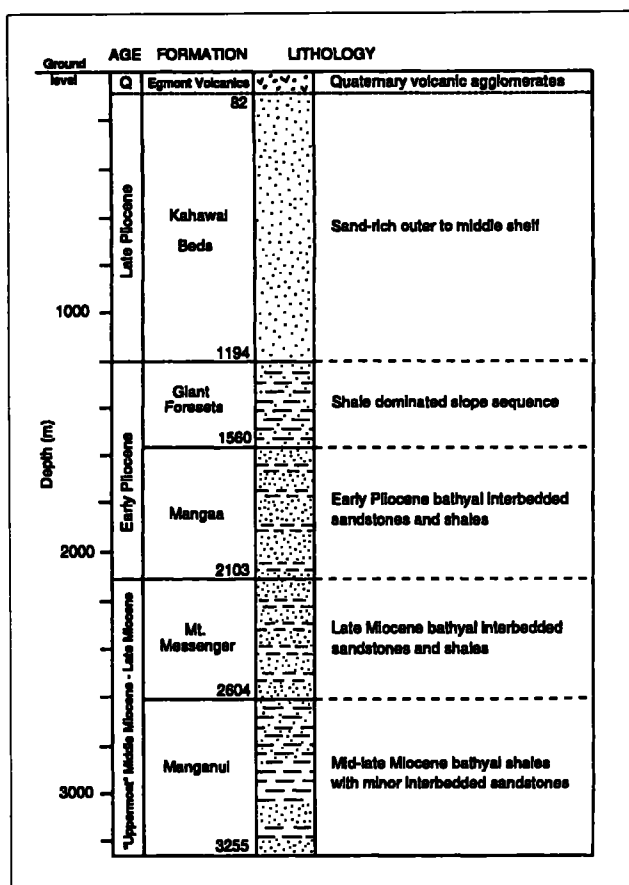


Fig. 2. Stratigraphy of Burgess-1 exploration well near Cape Egmont showing the units modelled in the synthetic seismograms.

The computations are made by computing the wave propagation through each layer of the model in the frequency-wave number domain. At the interfaces the partitioning of the wave fields is computed on the assumption of the continuity of deformation and fluid flow across the boundary. The internal reflections within the layers (or group of layers) is computed using the standard techniques of Kennett (1983). Because of the nature of sound waves in the porous media the velocities and attenuation of the various waves in each layer vary with frequency.

Physical parameters used in the modelling

For 2-D modelling there are eleven independent physical properties that need to be specified for each layer—5 elastic solid and 6 porosity and fluid properties (Bourbie et al, 1987).

Many of these parameters have been assumed constant for the modelling in this paper. Within the strata in the models in this paper the porosity range, viscosity of water and permeabilities are such that the critical frequencies ($\omega_c = \eta\phi/(\kappa\rho_s)$) are several kHz and so the slow compressional wave has little direct effect. Hence, the modelling is insensitive to variations in the viscosity of the fluid and the permeability of the sediments. In addition the high value of the critical frequency results in there being only minor variations of velocity for each material in the frequency ranges considered in this paper.

Table 2 shows the values of the physical parameters used in the numerical modelling. Many of the properties are poorly determined but some experiments using different values showed that the principles determined from the modelling held for a reasonable range of likely values.

In modelling the seismic response to the sand layers there are a range of options as to the behaviour of the material to the change in porosity. The two main options may be characterised by whether the compressibility of the sand grains (and the sands with all the water removed) remain the same or whether the bulk seismic velocities of the water-filled sands remains constant when there is no loss of water from the pores during the passage of the seismic wave.

For the synthetic shot records computed in this paper it has been assumed that the particle density of the sand material is constant (at 2600 kg/m³). Varying the porosity changes the bulk density. Two sets of synthetic models were then computed each with 2, 10, 25 and 40% porosity. For the first set the seismic velocity of the sands drained of all fluid was assumed constant. For the second set of synthetics, the seismic velocity at low frequency of the composite material, with the saturating fluid confined to remain within the solid matrix, is held constant. This corresponds to holding the velocity from sonic logs constant. Table 3 lists the relevant properties for the sand layer in the eight models used for the synthetic records in figures 3 and 4. For these the compressional wave velocity that is held constant has been

Table 2. Physical properties assumed for the various geological units (from well logs).

Geological Unit	P-velocity (km/s)	S-velocity (km/s)	Density* (Mg/m ³)	Porosity %	Permeability† (1.0 ⁻¹² m ²)
Volcanics	1.7	1.0	2.05	20	1.0
Upper Whenuahua	1.9	1.1	2.05	5	0.005–0.05
Lower Whenuahua	2.0	1.1	2.05	5	0.005–0.05
Tangahoe	2.8	1.6	2.25	2	0.005
Miocene Sands‡	3.2	1.8	2.20	25	1.0
Miocene Shales‡	3.2	1.8	2.30	2	0.005
Manganui	4.4	2.5	2.45	5	0.005
Fluid	density (Mg/m ³)		bulk modulus (10 ⁹ N/m ²)		viscosity (10 ³ kg/s/m)
Water	1.0		2.2		0.6

Notes

* S-velocity assumed to be 0.56*P-velocity

† 1.0⁻¹² m² = 1.0 Darcy

‡ These values from well logs but see table 3 for values for specific models

assigned a value equal to the sonic velocity measured in Burgess-1 and the shear wave velocity is computed assuming a Poisson's ratio of 0.25 for the solid matrix.

Results of modelling synthetic shot records

Figures 3 to 5 show the shot records (or CDP gathers) for several different models. The interfaces above the top of the sand layer (at 1800 m in the model) are the same in all the models. All the synthetics are computed for explosive sources, and with a shot to receiver offset range of -3 km to 0.5 km for both vertical and radial horizontal geophones. The true amplitudes calculated using the wave equation analysis have been adjusted using a cylindrical divergence correction (corresponding to a spherical divergence correction in 3-D) to uniformly increase the later arrivals at more distant geophones. It has been attempted to use the same gain for all plots — the similarity of the gain can easily be checked by comparing the amplitudes of the early arrivals on all the plots as they should be the same.

Figures 3a and 4a show the arrivals from the layers above the sand and can be used as a comparison with the other figures to indicate which arrivals are due to the sand layer. As expected there are clear compressional reflections from all the interfaces (indicated by high amplitudes on the vertical geophones at small offsets). However, there are also significant converted wave arrivals corresponding to compressional to shear wave conversions at nearly all the interfaces. These waves are identified by the two-way-travel-times and their lower apparent velocities.

Figures 3b-e show the effect of introducing a single 100 m thick layer of sand in the Mangaa part of the section (at 1800 m) under the assumption that the velocities of the sands drained of all fluids is independent of the porosity. This corresponds to the properties A-D in table 2 for porosities of 2, 10, 25, and 40% respectively. The compressional and converted wave arrivals from both the top and bottom of the sand layer are well developed. Again the compressional wave reflections are strongest where there is little offset between source and receiver. The converted wave amplitudes

are at a maximum with offsets between 1.0 and 2.5 km. The amplitudes of both the compressional and converted wave reflections vary markedly with the porosity, with the least amplitude being computed for the 10 and 25% porosity models. These are the models for which the densities used for the sands are closest to those of the shales. The bulk density of the sand changes from being greater than that of the shale at 10% porosity to less than the shales at 25% porosity. As a consequence the polarity of the reflections also changes in the synthetics for these porosities.

The effect of changing the porosity while maintaining the seismic velocity of the sands with confined water (properties E-H in Table 2) is shown in figure 4. As for figure 3 the main differences caused by changes in the porosity are in the amplitude of the reflections.

In both figure 3 and 4 the effect of changes in the porosity on the physical properties of the sands were assumed to be in the compressional and shear velocities. However, the method of calculating these velocities resulted in the ratio of the compressional and shear velocities remaining almost constant, being equivalent to a Poisson's ratio of about 0.25. Figure 5 illustrates the effect of varying the Poisson's ratio for the matrix material while holding the porosity and compressional velocity of the sands constant. This results in changes in the shear velocity. As for figures 3 and 4 the top synthetic shot in figure 5, for a model with no sand layers, is included so that the effects of the sand layer can be determined in the lower shots. The second synthetic shot (figure 5b) is for a Poisson's ratio of 0.25 for all the units, the third (figure 5c) has a Poisson's ratio of 0.35 for the shales and sands while the last has a Poisson's ratio of 0.4 for the shales and 0.35 for the sand layer. The differences in the reflections are evident on both the compressional wave reflection (principally on the vertical geophones) and on the converted waves (principally on the horizontal geophones). This part of the analysis shows that the variation in Poisson's ratio has a much greater effect on the offsets at which the reflections from the sands are a maximum than the variations in porosity, as shown in figures 3 and 4.

Table 3. Properties of Miocene Sands used for synthetic models.

Model	Porosity %	pshell kg/m ³	pwet kg/m ³	V _o m/s	S _o m/s	V _r m/s	S _r m/s	ω _c kHz
<i>Solid matrix material held constant</i>								
A	2	2548	2570	3200	1800	3190	1795	2
B	10	2340	2440	3200	1800	3155	1765	10
C	25	1950	2200	3200	1800	3060	1700	24
D	40	1560	1960	3200	1800	2900	1580	38
<i>Velocity of the composite material at low frequency held constant</i>								
E	2	2548	2570	3210	1810	3200	1800	2
F	10	2340	2440	3250	1840	3200	1800	10
G	25	1950	2200	3350	1910	3200	1800	24
H	40	1560	1960	3510	2020	3200	1800	38

Notes:

- pshell Density of evacuated porous shell (shell material has density of 2600 kg/m³)
- pwet Density of saturated porous shell
- V_o Compressional seismic velocity of empty shell
- S_o Shear seismic velocity of empty shell
- V_r Compressional seismic velocity with confined fluid
- S_r Shear seismic velocity with confined fluid
- ω_c Critical frequency

CONSTANT MATRIX VELOCITY

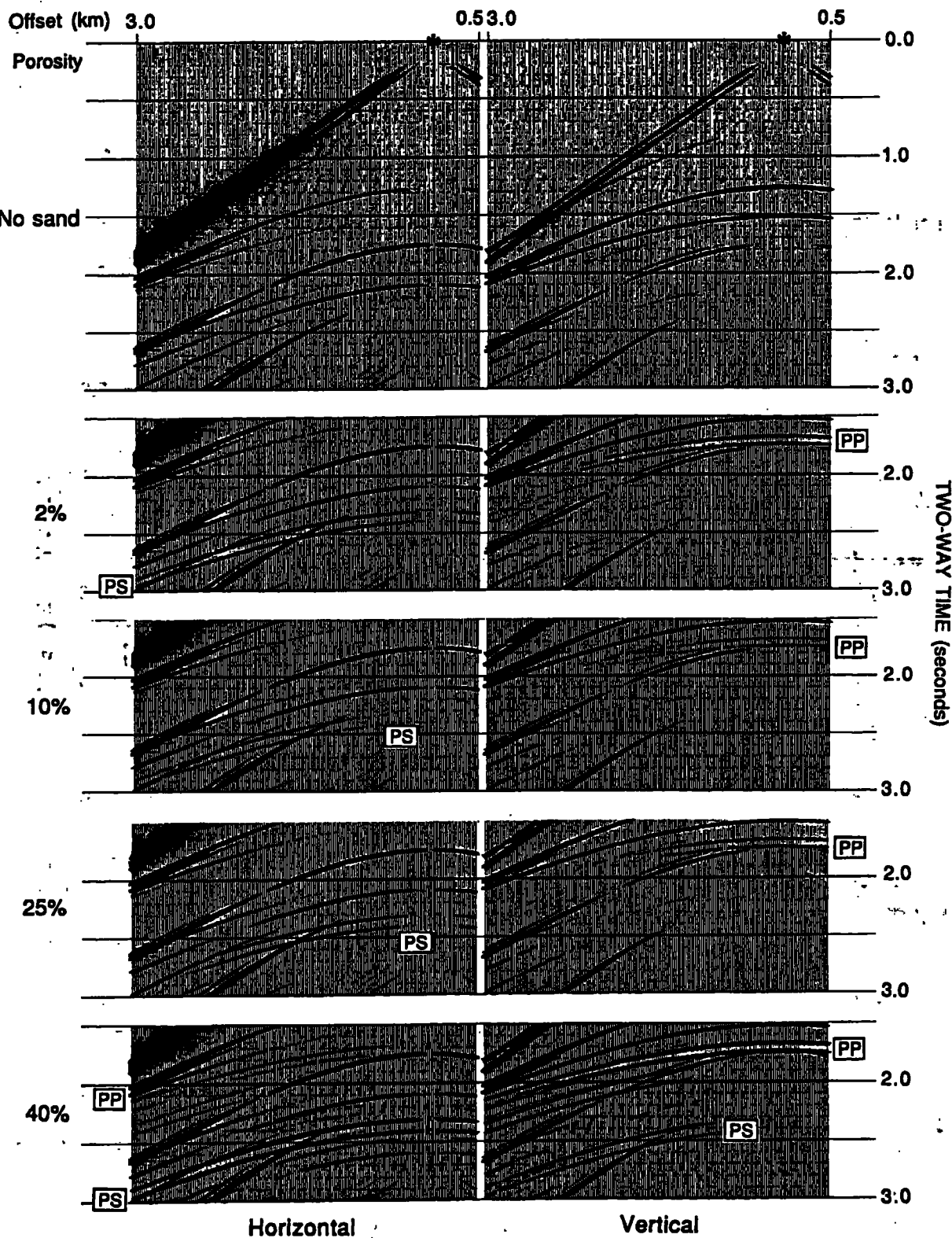


Fig. 3. Synthetic shot records for models incorporating a 100 m sand layer with various porosities, and in which the seismic velocity of the sand matrix is kept constant. The physical properties of the layers are given in tables 2 and 3. PP indicates compressional wave reflection and PS indicates converted wave reflection.

Walkout Test

A two-component walkout test was recorded on 24 June 1993. The location of the test, along Pungarehu Road, Cape

Egmont, (figure 1) was chosen for several reasons. The Pliocene-Miocene shale-sand sequence was quite well established from previous seismic recording and the Burgess-1

CONSTANT VELOCITY WHEN FLUIDS ARE CONFINED

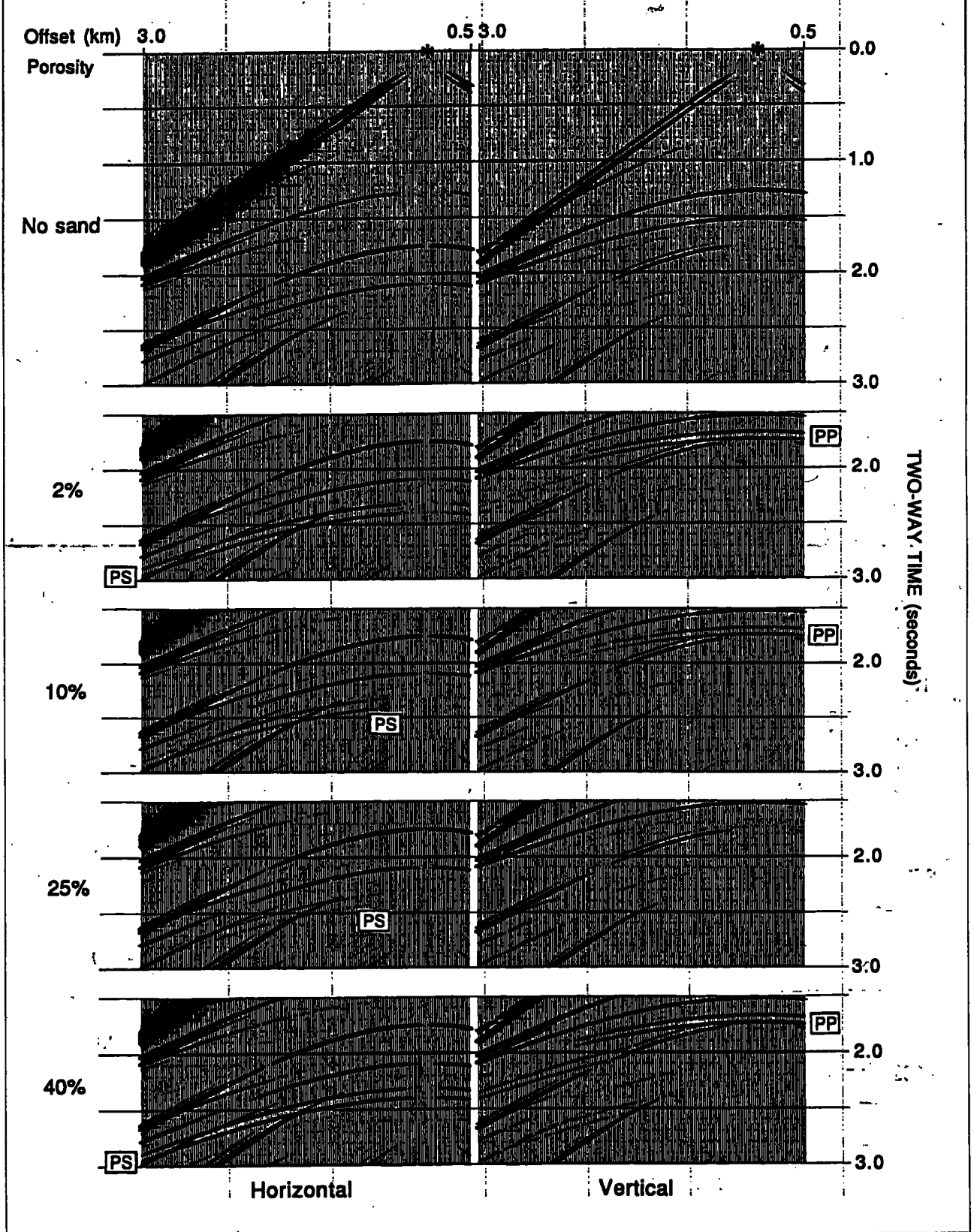


Fig. 4. Synthetic shot records for models incorporating a 100 m sand layer with various porosities, and in which the seismic velocity of saturated sands with the water contained within its volume is kept constant. The physical properties of the layers are given in tables 2 and 3. PP indicates compressional wave reflection and PS indicates converted wave reflection.

well. The line was oriented in the strike direction so that the stratigraphic boundaries would be flat lying images on the seismic section. There was adequate drill control from the

Burgess-1 exploration well. The area is also known to be one in which existing seismic records are clear and of excellent quality. This is in marked contrast to other locations, such as

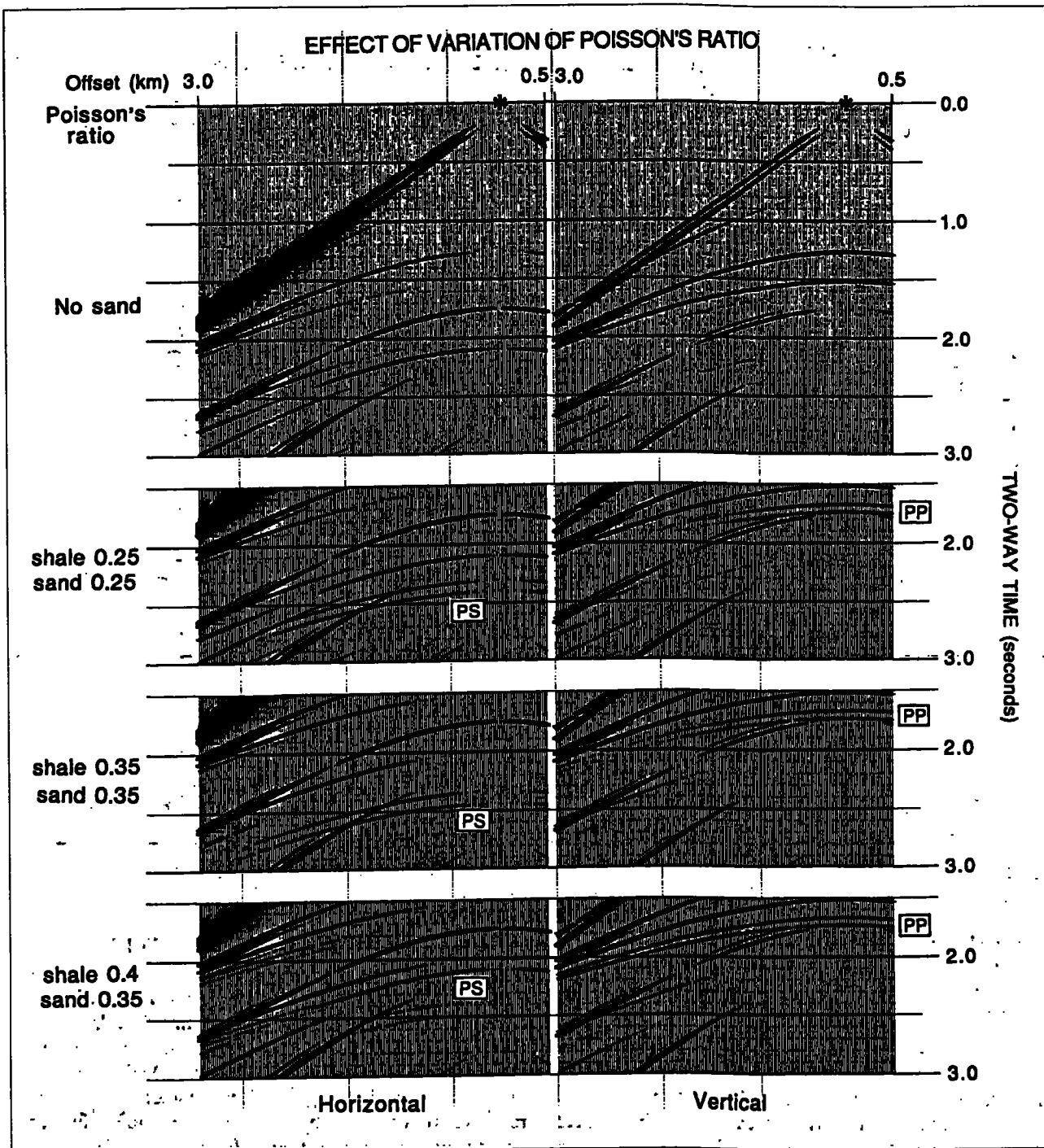


Fig. 5. Synthetic shot records for models incorporating a 100 m sand layer with 25% porosity. For the top shot the Poisson's ratio is 0.25 for all layers. (This is identical to the 25% porosity records in figure 3). The second shot has the Poisson's ratio increased to 0.35 while the third record has the Poisson's ratio of the sand equal to 0.35 and the other layers as 0.4. PP indicates compressional wave reflection and PS indicates converted wave reflection.

northeast of Mt Taranaki where there is better well control but seismic data is of poor quality because of the variable thickness of the surficial lahar deposits.

The data were recorded on the Institute's 48 channel SERCEL 338HR with a stationary geophone spread consisting of 24 three component geophones (of which only the vertical and inline-horizontal components were recorded). The geophones which had a 10 Hz natural frequency, were spaced at 10 m.

The 16 seismic sources (approximately 2 kgs of Power-Gel set at 5 m depth and tamped with pea gravel) were shot at approximately 230 m intervals starting 245 m west of the

western-most geophone. By appropriately sorting the resulting traces the equivalent of a 3550 m long spread was recorded with the maximum offset between the shot and receiver being 470 m to the west and 3080 m to the east.

Shot records were displayed with the horizontal and vertical components separated and the traces reordered into ascending offset. So that the scale could be the same as that of the synthetic records already discussed, the data from every second geophone are displayed giving a 20 m spacing between traces.

Spherical divergence gain was applied to the traces, which were then filtered with a 15-85 Hz bandpass filter and

